3010–3016 *Nucleic Acids Research, 1996, Vol. 24, No. 15*

Selection of the best target site for ribozyme-mediated cleavage within a fusion gene for adenovirus E1A-associated 300 kDa protein (p300) and luciferase

Hiroaki Kawasaki[1–3], Jun Ohkawa[1], Norie Tanishige[1,3], Koichi Yoshinari[1], Takehide Murata[2], Kazunari K. Yokoyama[2] and Kazunari Taira[1,3,*]

[1]National Institute of Bioscience and Human Technology, Agency of Industrial Science and Technology, MITI, [2]Tsukuba Life Science Center, The Institute of Physical and Chemical Research (RIKEN), 3-1-1 Koyadai and [3]Institute of Applied Biochemistry, University of Tsukuba, Tennoudai 1-1-1, Tsukuba Science City 305, Japan

Received March 22, 1996; Revised and Accepted June 18, 1996

ABSTRACT

The cellular 300 kDa protein known as p300 is a target for the adenoviral E1A oncoprotein and it is thought to participate in prevention of the G_0/G_1 transition during the cell cycle, in activation of certain enhancers and in the stimulation of differentiation pathways. In order to determine the exact function of p300, as a first step we constructed a simple assay system for the selection of a potential target site of a hammerhead ribozyme *in vivo*. For the detection of ribozyme-mediated cleavage, we used a fusion gene (*p300–luc*) that consisted of the sequence encoding the N-terminal region of p300 and the gene for luciferase, as the reporter gene. We were also interested in the correlation of the GUX rule, for the triplet adjacent to the cleavage site, with ribozyme activity *in vivo*. Therefore, we selected five target sites that all included GUX. The rank order of activities *in vitro* indeed followed the GUX rule; with respect to the k_{cat}, a C residue as the third base (X) was the best, next came an A residue and a U residue was the worst (GUC > GUA > GUU). However, *in vivo* the $tRNA^{Val}$ promoter-driven ribozyme, targeted to a GUA located upstream of the initiation codon, had the highest inhibitory effect (96%) in HeLa S3 cells when the molar ratio of the DNA template for the target p300 RNA to that for the ribozyme was 1:4. Since the rank order of activities *in vivo* did not conform to the GUX rule, it is unlikely that the rate limiting step for cleavage of the *p300–luc* mRNA was the chemical step. This kind of ribozyme expression system should be extremely useful for elucidation of the function of p300 *in vivo*.

INTRODUCTION

Elucidation of the functions and the site of interaction with their targets of transcription factors is of considerable current interest (1–3). A 300 kDa cellular protein, known as p300, is a nuclear phosphoprotein that is the binding target of the adenovirus E1A oncoprotein (4). The region of E1A required for binding of p300 includes residues at the N-terminus and in CR1 (conserved region 1) of the E1A oncoprotein (5). Binding of p300 to E1A is believed to stimulate the G_0/G_1 transition, to block differentiation and to inhibit the action of certain transcriptional enhancer elements (5). Other data support the view that p300 plays a role as a co-activator (6–12) and the p300 protein has been shown to activate transcription when fused to a DNA binding domain (7,8). However, the functional significance of p300 protein *in vivo* is still unknown. Thus, we decided to construct a system in which expression of p300 was regulated by a hammerhead ribozyme.

Recently, regulation of gene expression by ribozyme and antisense RNA/DNA has been performed (13–17). The principle of catalytic self-cleavage of RNA molecules and of cleavage in *trans* has been well established over the last decade (18). Expression of various genes has been suppressed by ribozymes (13–21) and among the RNA molecules with ribozyme activity, the hammerhead ribozyme is the best characterized (22–28). It is well established that ribozymes require divalent metal ions for cleavage activity *in vitro* and *in vivo* (29–38). Theoretically, it is possible for one molecule of ribozyme to cleave multiple target RNAs. On the other hand, for high level activity, an antisense RNA needs a cellular factor, such as an RNase III-type nuclease, to destroy the target RNA. As a consequence, a ribozyme tends to show a higher inhibitory effect than does an antisense RNA (39).

The activity of ribozymes depends very strongly on the target site and, furthermore, it is not easy to predict the best cleavable target site. Both primary (40–43) and secondary structural rules (44) must be considered in selection of the target site. In general, the GUC triplet should be suitable as a cleavage site, since it conforms to the NUX rule, where N is A, U, G or C and X is A, U or C (40–47), and since it is the most popular triplet used in nature (24, 43). In addition, the tertiary structure of the target RNA *in vivo* (including interaction with cellular proteins) should also be considered in selecting the target site, since it has a strong influence on the activity of ribozymes and antisense molecules. Unfortunately, it is difficult to predict the *in vivo* tertiary structure of the cleavage site, even though the selected site is in accord with

*To whom correspondence should be addressed at: Institute of Applied Biochemistry, University of Tsukuba, Tennoudai 1-1-1, Tsukuba Science City 305, Japan

the primary and secondary structural rules. As a result, selection of the best target site remains a matter of trial and error.

Another challenge for *in vivo* application of ribozymes is construction of a gene for a ribozyme that allows continuous expression of the ribozyme in a particular cell. Despite an increasing number of successful studies, based on general rules for antisense sequences and on sophisticated constructs for the expression of ribozymes, the design of ribozymes that cleave RNA *in vivo* is also a matter of trial and error.

Our previous kinetic studies *in vitro* demonstrated that in reactions catalyzed by a *trans*-acting hammerhead ribozyme, mutant substrates that contained a GUA or GUU triplet at the cleavage site were cleaved less efficiently than a wild-type substrate with the GUC triplet (42). For our analysis of the function of p300 using a ribozyme that would significantly suppress expression of p300 *in vivo*, we needed an appropriate combination of a good target site and a ribozyme expression system. We chose luciferase activity as a reporter and linked the sequence that encoded the N-terminal region (285 nt in length) of p300 to the gene for luciferase. In general, the N-terminal region is the first choice for the target site of ribozymes and antisense molecules (39). We were also interested in the correlation of the GUX (X = A, U or C) rule, derived on the basis of studies *in vitro* (42), with ribozyme activity *in vivo*. Therefore, we chose five different target sites which contained the GUC, GUA or GUU triplet within this N-terminal region and the efficiency of cleavage at each site was examined *in vitro* and *in vivo* in a transient co-transfection assays in HeLa S3 cells.

We report here that all ribozymes whose synthesis was driven by the $tRNA^{Val}$ promoter significantly suppressed expression of the *p300–luc* fusion gene, with the exception of the inactive ribozyme control. Since the inactive ribozyme control did not have any inhibitory effect, the observed activities appeared to originate from the cleavage activities of the ribozymes. Moreover, since the rank order of activities *in vivo* did not conform to the recently established GUX rule (41,42), it is unlikely that the rate limiting step for cleavage of the *p300–luc* mRNA *in vivo* was the chemical step. Most importantly, in this study a significant inhibitory effect was observed when the molar ratio of the DNA template for the target *p300* mRNA to that for the ribozyme was only 1:1. Therefore, this kind of ribozyme system should be a useful tool to elucidate the function of p300 *in vivo*.

MATERIALS AND METHODS

Synthesis of oligonucleotides, ribozymes and substrates

Oligonucleotides were synthesized with a DNA/RNA synthesizer (model 392; Applied Biosystems, Foster City, CA) and purified on OPC columns. Ribozymes and their corresponding substrates used for kinetic measurements *in vitro* were synthesized with a DNA/RNA synthesizer (model 392; Applied Biosystems) and purified by polyacrylamide gel electrophoresis as described previously (36,38,42,48,49). Reagents for manipulation of RNA were purchased from either ABI or American Bionetics Inc. (ABN; Foster City, CA). Sequences of the synthetic ribozymes and their corresponding substrates were as follows: Ribozyme 1 (R1), 5′-GAG GAA CUG AUG AGG ACC GAA AGG UCG AAA CCA GA-3′; Ribozyme 2 (R2), 5′-CGG AGA CUG AUG AGG ACC GAA AGG UCG AAA CAA GC-3′; Ribozyme 3 (R3), 5′-CUG GCG CUG AUG AGG ACC GAA AGG UCG AAA CGC CG-3′; Ribozyme 4 (R4), 5′-UGC CAA CUG AUG AGG ACC GAA AGG UCG AAA CUU GU-3′; Ribozyme 5 (R5), 5′-AUC UUG CUG AUG AGG ACC GAA AGG UCG AAA CCA UG-3′; Substrate 1 (S1), 5′-UCU G**GU U**UU CCU C-3′; Substrate 2 (S2), 5′-GCU U**GU A**UC UC CG-3′; Substrate 3 (S3), 5′-CGG C**GU C**CG CCA G-3′; Substrate 4 (S4), 5′-ACA A**GU C**UU GGC A-3′; Substrate 5 (S5), 5′-CAU G**GU A**CA AGA U-3′.

Kinetic measurements *in vitro*

Reaction rates *in vitro* were measured at 37°C in 10 mM $MgCl_2$ and 50 mM Tris–HCl, pH 6.0, under ribozyme saturating (single turnover; the final concentration of each ribozyme was 100 nM) conditions with 5′-^{32}P-labeled substrate (the final concentration of each substrate was 10 nM). Reactions were stopped by removal of aliquots from the reaction mixture after 10 min incubation and mixing with an equivalent volume of a solution of 100 mM EDTA, 9 M urea, 0.1% xylene cyanol and 0.1% bromophenol blue. Substrates and 5′-cleaved products were separated by electrophoresis on a 20% polyacrylamide–7 M urea denaturing gel and were detected by autoradiography (Fig. 2). The extent of cleavage was determined by quantitation of radioactivity in the bands of the substrate and product with a Bio-Image Analyzer (BA2000; Fuji Film, Tokyo).

Construction of a plasmid for expression of the *p300–luc* fusion gene

For the detection of ribozyme-mediated cleavage, we used a fusion gene (*p300–luc*) that consisted of the sequence encoding the N-terminal region of p300 and the gene for luciferase, as the reporter gene. The plasmid for expression of the *p300–luc* fusion gene was constructed from the Pica Gene™ Luciferase Control Vector (Control Vector; Toyoinki, Tokyo). In brief, the DNA fragment encoding the N-terminal region of p300 (nt 1146–1430) was amplified from pCMVb p300 (6) by PCR with 5′-AAT TCG ATA AGC TTG AGA TTT CCT GAG GAT TCT GGT TTT-3′ as the 5′ primer and 5′-TAG GCC GCT CTA GAG GAT AGA ATG GCG CCG GGC CTT TCT TTA TGT TTT TAG AAG CTG CAT CTT GTA CCA TG-3′ as the 3′ primer. After digestion with *Hin*dIII and *Xba*I, this fragment was inserted into the *Hin*dIII and *Xba*I sites of the Control Vector. The nucleotide sequence of the *p300–luc* fusion gene was confirmed by sequencing.

Construction of plasmids for expression of a hammerhead ribozyme and antisense RNA

Chemically synthesized oligonucleotides encoding ribozyme 2, inactive ribozyme 2 or antisense 2 (Fig. 1C) and the pol III termination sequence (50) were convered to double-stranded sequences by PCR. After digestion with *Csp*45I and *Sal*I, the fragments were cloned downstream of the tRNA promoter of pUC-tRVP (which contains the chemically synthesized promoter for human $tRNA^{Val}$ between the *Eco*RI and *Sal*I sites of pUC19). The sequences of all constructs were confirmed by direct sequencing.

Cell culture and transfection

HeLa S3 cells were cultured in Dulbecco's modified Eagle's medium containing 10% (v/v) fetal bovine serum, 100 µg/ml penicillin and 100 µg/ml streptomycin. Transfections with plasmid DNA were performed using Lipofectin (Gibco BRL, Gaithersburg,

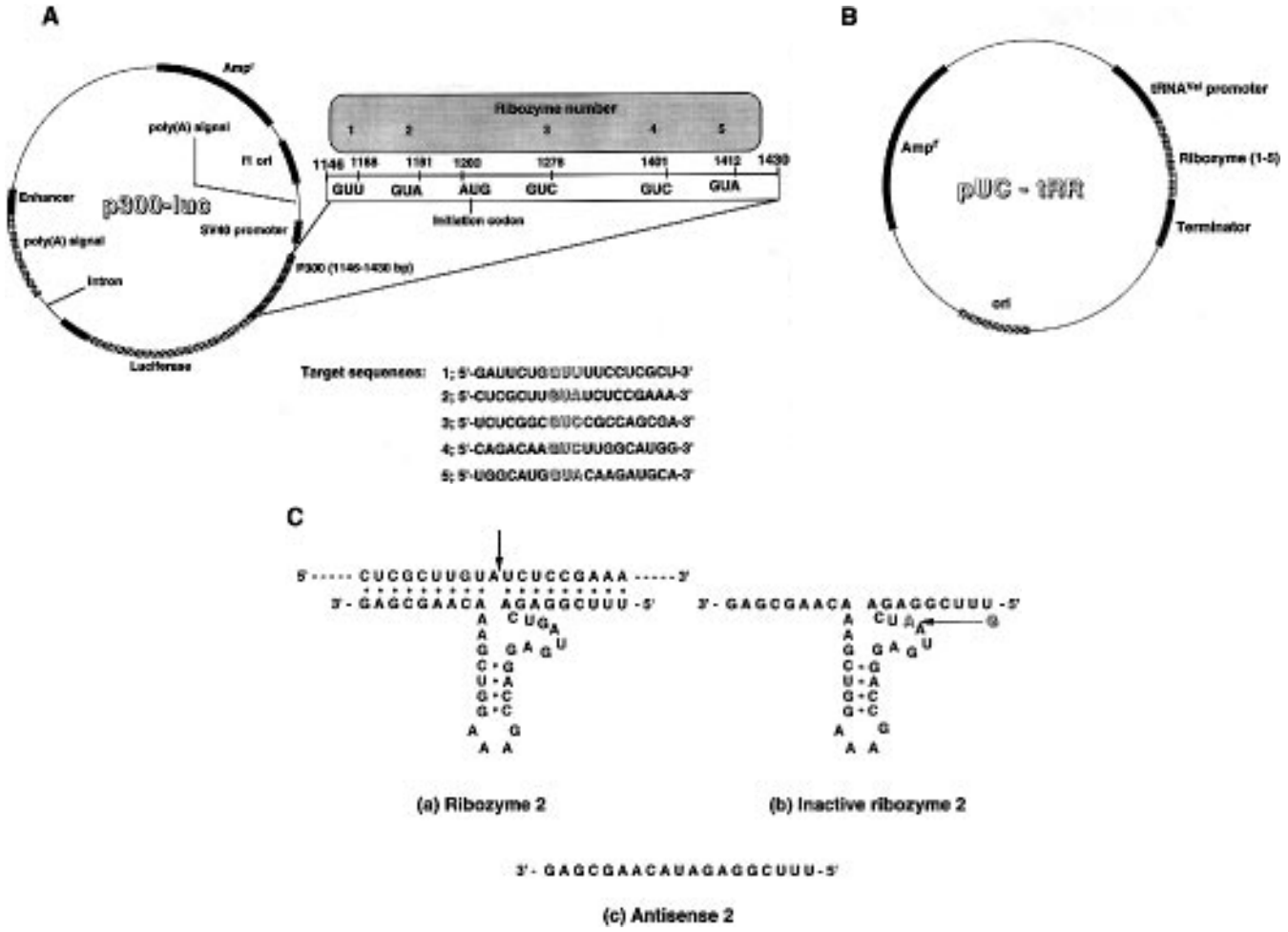

Figure 1. (**A**) Construction of plasmids that contained *p300–luc* fusion genes and the location of the target sites relative to the gene for p300. Positions of target sites, including the triplets of each ribozyme, numbered 1–5, are indicated by vertical lines on the open box on the left. The initiation codon (AUG) is indicated at nt 1200. Target sequences are listed at the bottom. (**B**) Plasmid pUC-tRR, which contains a $tRNA^{Val}$-driven ribozyme, 1–5. The ribozyme clones are represented schematically, where 'Ribozyme' designates the short region complementary to the target gene for p300 that incorporates the catalytic loop of the ribozyme. Each plasmid contained a ribozyme targeted to a different region of the p300 transcript [target sites are indicated in (A)]. (**C**) Secondary structures of ribozyme 2 and inactive ribozyme 2 and the sequence of antisense 2. (a) Predicted secondary structure of the catalytic loop of ribozyme 2, also showing ribozyme–substrate complementarity; the arrow indicates the cleavage site. The active ribozyme includes a wild-type ribozyme sequence. (b) Inactive ribozyme 2 has a single G5→A5 substitution in the catalytic domain. (c) The antisense 2 molecule that served as a control.

MD) in accordance with the manufacturer's protocol. In brief, 3×10^5 cells were plated in 6-well plates 1 day before transfection. After cells had been washed twice with phosphate-buffered saline (PBS), 0.8 ml OPTI-MEM I medium (Gibco BRL) was added to each well. A solution of plasmid DNA (6 µg plasmid DNA in 100 µl OPTI-MEM I medium) and a solution of Lipofectin (4 µl Lipofectin reagent in 100 µl OPTI-MEM I medium) were mixed gently and the mixture was kept at room temperature for 20 min to allow formation of Lipofectin–DNA complexes. The solution of Lipofectin–DNA complexes was added to the cells. After 12 h, the medium was removed and 2 ml of the growth medium were added. The cultures were incubated for an additional 24 h.

Measurement of luciferase activity

Transfected cells were washed twice with PBS and lysed in lysis buffer (Tris–PO_4, pH 7.8, 8 mM $MgCl_2$, 1 mM DTT, 1 mM EDTA, 1% Triton X-100, 1% BSA and 15% glycerol). After removal of cell debris by centrifugation in a microcentrifuge, the luciferase activity in the supernatant was measured by the method of Alam and Cook (51). One hundred microliters of luciferase assay reagent [20 mM Tricine, 1.07 mM $(MgCO_3)_4Mg(OH)_2{\cdot}5H_2O$, 2.67 mM $MgSO_4$, 0.1 mM EDTA, 33.3 mM dithiothreitol, 270 µM coenzyme A, 470 µM luciferin and 530 µM ATP] were added to 20 µl of the supernatant in a test tube. The integrated light output was measured with a luminometer (Lumat LB9501; Berthold, Bad Wildbad, Germany).

Northern blot analysis

Total cellular RNA was isolated from transfected cells as described by Chomczynski and Sacchi (52). RNA (10 µg), denatured with glyoxal (53), was fractionated on a 2.2% agarose gel, transferred to a nylon membrane (Hybond-N; Amersham, UK) and allowed to hybridize with a 5′-^{32}P-end-labeled oligonucleotide probe (5′-CTC GCT TGT TTC GGA CCT TT-3′,

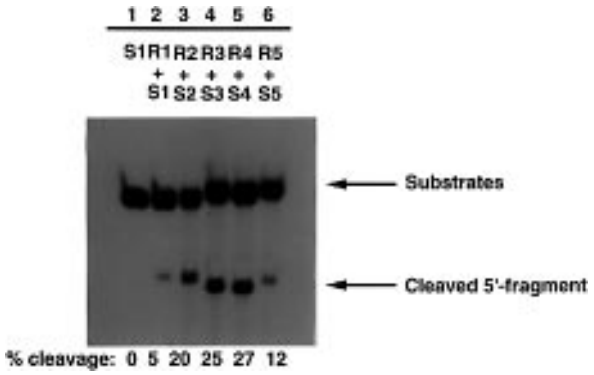

Figure 2. Relative activities of synthetic ribozymes. The autoradiogram represents the ribozyme-mediated cleavage of the corresponding substrate. Reactions were carried out *in vitro* at 37°C for 10 min in 10 mM $MgCl_2$ and 50 mM Tris–HCl, pH 6.0, under ribozyme saturating (single turnover) conditions (the final concentration of each ribozyme was 100 nM) with 5′-^{32}P-labeled substrate (the final concentration of each substrate was 10 nM). The extent of cleavage (%) in 10 min was determined by quantitation of radioactivity in the bands of the substrate and the cleaved 5′-fragment with a Bio-Image Analyzer (BA2000; Fuji Film, Tokyo). The complete sequences of the ribozymes and substrates used are listed in Materials and Methods.

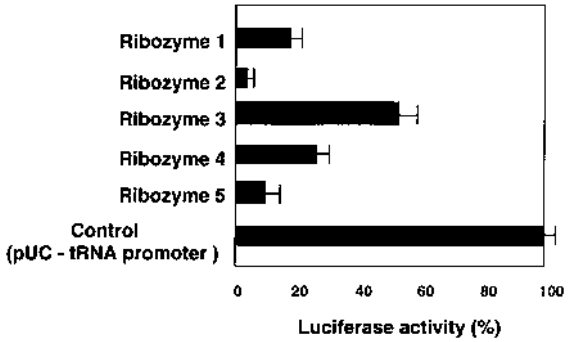

Figure 3. Effect of ribozymes on expression of the *p300–luc* fusion gene. The effects of ribozymes on expression of the *p300–luc* fusion gene in HeLa S3 cells co-transfected with pUC-tRR at 4 µg/dish and *p300–luc* at 2 µg/dish (see text for details). The results shown are averages of results from five sets of experiments and are given as percentages relative to the control value of 100% (pUC-tRVP). The absolute value in light units of the control (pUC-tRVP) was ~520 000.

specific for ribozyme 2 and inactive ribozyme 2, or 5′-CTC GCT TGT ATC TCC GAA A-3′, specific for antisense 2; Fig. 1C).

RESULTS AND DISCUSSION

Construction of a plasmid (*p300–luc*) that encodes the N-terminal region of p300 and luciferase

The exact function of the cellular protein p300 remains obscure. In order to suppress the expression of p300, we tried to identify the best target site within the p300 transcript for ribozyme-mediated cleavage. Since the phenotype of suppressed p300 clones cannot be used for quantitation of the efficiency of ribozyme-mediated cleavage and, moreover, since the cleavage products, in general, cannot be detected *in vivo*, we constructed a rapid assay system for selection of the best target site by fusing the N-terminal region of the gene for p300 (corresponding to nt 1146–1430, according to the numbering of Eckner *et al.*; 6) in-frame with the gene for luciferase (Fig. 1A). The fused gene product was produced under the control of the SV40 promoter and its enhancer.

Construction of pol III-driven ribozyme and antisense expression plasmids

In a previous study, we examined the generality of the NUX rule (where N is A, U, G or C and X is A, U or C) and we demonstrated from kinetic studies *in vitro* that in reactions catalyzed by *trans*-acting hammerhead ribozymes, mutant substrates that contained the GUA or GUU triplet were cleaved less efficiently than the wild-type substrate with the GUC triplet (GUG could not be cleaved; 42). In choosing potential target sites for examination of the efficiency of their ribozyme-mediated cleavage *in vivo*, we made sure that each of the selected conserved sites contained one of all possible GUX triplets.

The five selected target sites are indicated in Figure 1A and the corresponding ribozymes are numbered 1–5 in the upstream to downstream direction. Each of the ribozymes was transcribed under the control of the human $tRNA^{Val}$ promoter (Fig. 1B). Each ribozyme had the same 24 nt catalytic domain as that refined by Haseloff and Gerlach (43) and each was equipped with nine bases on both substrate binding arms that were targeted to the relatively well-conserved sequences of p300 mRNA.

Since ribozyme 2 targeted to the GUA site was found to be the most active (see below), constructs with an inactive ribozyme and an antisense control targeted to the same site were generated (Fig. 1C). The inactive ribozyme differed from the active ribozyme by a single $G_5 \rightarrow A$ mutation in the catalytic core (the numbering system follows the rule for hammerhead ribozymes; 54). This single base change should diminish the cleavage activity while the antisense effect, if any, should be unaffected (39,40). As a second control for comparison of the activity of ribozyme 2 with that of an antisense RNA, we synthesized an antisense construct in which the entire catalytic domain of ribozyme 2 was replaced by a single uracil moiety (Fig. 1C).

Re-examination of the GUX rule *in vitro*

In a previous study, in order to examine in detail the generality of the NUX rule for the GUC triplet adjacent to the cleavage site in hammerhead ribozymes, kinetic parameters were determined for substrates with mutations only within this triplet (42). In the present study, sequences of the selected five target sites differed not only in the GUX triplet, but also in the binding sites. In order to examine whether activities *in vitro* of the five ribozymes selected in this study might follow the GUX rule, we chemically synthesized five ribozymes (R1–R5) and their corresponding substrates (S1–S5) and relative activities were measured under single turnover conditions. In this case, each synthetic ribozyme was equipped with six bases on both substrate binding arms (complete sequences are listed in Materials and Methods).

Results of such studies are shown in Figure 2. The level of cleavage (%) in 10 min in 10 mM $MgCl_2$ and 50 mM Tris–HCl, pH 6.0, at 37°C was 5, 20, 25, 27 and 12% respectively, for R1/S1 (GUU), R2/S2 (GUA), R3/S3 (GUC), R4/S4 (GUC) and R5/S5 (GUA). The order of efficiency of cleavage was as follows: R4 (GUC) > R3 (GUC) > R2 (GUA) > R5 (GUA) > R1 (GUU), where the target triplet is indicated in parentheses. Therefore, the

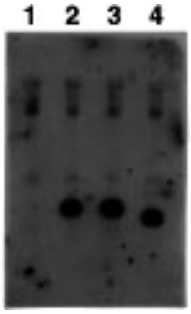

Figure 4. Expression *in vivo* of ribozymes and antisense RNA, as monitored by Northern blot analysis. Lane 1, total RNA in HeLa cells; lane 2, inactive ribozyme 2; lane 3, ribozyme 2; lane 4, antisense 2.

rank order of activities *in vitro* followed the GUX rule; a C residue as the third base (X) was the best, next came an A residue and a U residue was the worst (GUC > GUA > GUU).

Suppression of expression of the *p300–luc* fusion gene: results of transient transfection assays

The effects of the ribozymes, produced in *trans*, on the specific target mRNA, namely the transcript of the *p300–luc* fusion gene, were examined by measuring luciferase activity in HeLa S3 cells that had been co-transfected with the plasmids that encode the ribozymes and the *p300–luc*iferase (pUC-tRR and p300-luc plasmids respectively). To determine the effectiveness of ribozyme-mediated inhibition of expression of the *p300–luc* fusion gene in the transient expression assay, a control plasmid (pUC-tRVP), namely pUC-tRR from which the ribozyme sequence had been deleted (Fig. 1B), was used to allow generation of luciferase activity that was designated 100%. As shown in Figure 3, all the active ribozymes were capable of decreasing luciferase activity *in vivo*. The results shown are averages of results from five sets of experiments and are given as percentages relative to the control value of 100%. The extent of inhibition by ribozymes expressed from the pol III promoter varied from 47 to 96% when the molar ratio of template DNAs for the target and the ribozyme was 1:4. To the best of our knowledge, this is the lowest ratio ever reported to yield a significant inhibitory effect and it proves the utility of the pol III promoter in mammalian cells (55,56).

The order of efficiency of cleavage was as follows: R2 (GUA) > R5 (GUA) > R1 (GUU) > R4 (GUC) > R3 (GUC), where the target triplet is indicated in parentheses. These results would not have been predicted from the cleavage activity of NUX triplets in the *trans* system (42; Fig. 2) and they suggest, in turn, that accessibility of the target site governs the effectiveness of the ribozyme. Since the accessibility of the target site is not easily predictable, the generation of ribozymes that cleave RNA *in vivo* remains, unfortunately, a matter of trial and error. However, a system for the rapid evaluation of ribozyme activity *in vivo*, such as the one described herein, is of obvious value.

Ribozyme specificity in the suppression of expression of the *p300–luc* fusion gene

Since ribozyme 2 was found to be the most effective ribozyme (Fig. 3), we examined its antisense effect using the inactive ribozyme control. Furthermore, the inhibitory effect of the ribozyme

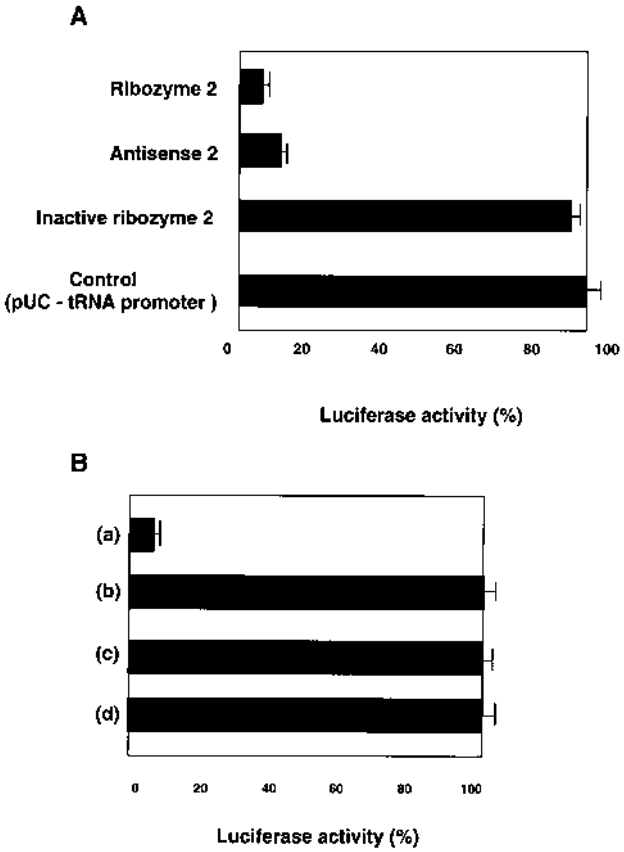

Figure 5. (**A**) Effects of ribozyme 2, of antisense 2 and of inactive ribozyme 2 on expression of the *p300–luc* fusion gene. The effects of ribozyme 2, of antisense 2 and of inactive ribozyme 2 on expression of the *p300–luc* fusion gene in HeLa S3 cells co-transfected with pUC-tRR at 4 µg/dish and *p300–luc* at 2 µg/dish are shown (see text for details). The results shown are averages of results from five sets of experiments and are given as percentages relative to the control value of 100% (pUC-tRVP). (**B**) Suppression of expression of the *p300–luc* fusion gene and of a gene for luciferase (Pica Gene™ Luciferase Control Vector) by ribozyme 2. The effects of ribozyme 2 on expression of the *p300–luc* fusion gene and the gene for luciferase in HeLa S3 cells co-transfected with pUC-tRR at 4 µg/dish and *p300–luc* or the Pica Gene™ Luciferase Control Vector at 2 µg/dish are shown (see text for details). Lane a, suppression of expression of the *p300–luc* fusion gene by ribozyme 2; lane b, suppression of expression of the *p300–luc* fusion gene by control vector (pUC-tRVP); lane c, suppression of expression of a gene for luciferase by ribozyme 2; lane d, suppression of expression of a gene for luciferase by control vector (pUC-tRVP).

was compared with that of antisense RNA targeted to the same site. Since the antisense RNA was significantly shorter than the ribozyme, levels of expression of ribozyme 2, inactive ribozyme 2 and antisense 2 RNA were examined by Northern blotting (Fig. 4). The levels of expression were determined by quantitation of the radioactivity of bands with an image analyzer. The levels of expression were found to be nearly identical in each of the three cases, within the limits of experimental error (Fig. 4).

The three constructs were examined for their ability to suppress expression of the *p300–luc* fusion gene, as described in the previous section. As shown in Figure 5A, the inactive ribozyme did not have any inhibitory effect, in accord with our previous finding in a bacterial system (39). The expected stability of RNA duplexes is as follows: antisense > inactive ribozyme ≈ active

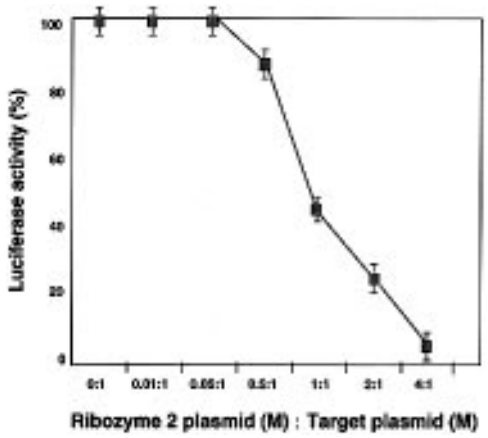

Figure 6. Effects of the amount of ribozyme expression plasmid on expression of the *p300–luc* fusion gene. The effects of the amount of ribozyme 2 on expression of the *p300–luc* fusion gene in HeLa S3 cells co-transfected with pUC-tRR at 0.01–4 μg/dish and *p300–luc* at 2 μg/dish are shown (see text for details). Relative ratios are indicated by molar ratios.

ribozyme. The significant inhibition by the antisense RNA was in accord with this prediction. Moreover, the RNase III-type activity of the host cells should increase the inhibitory effect of the antisense RNA. Since the inactive ribozyme (which, with its target site duplex, would not be expected to be a substrate for RNase III-type ribonucleases because of the discontinuous base pairing) did not have any inhibitory effect, it seems likely that the inhibitory effects of the ribozyme originated from its cleavage activity.

The suppressive effects of the ribozyme constructs on luciferase activity were apparently specific. To confirm the specificity of the ribozyme, an independent reporter gene, namely the gene for luciferase without the region that encoded the N-terminal sequence of p300 (Pica Gene™ Luciferase Control Vector) under the control of the SV40 promoter, was also used to co-transfect HeLa S3 cells. The luciferase activity (%) is shown in Figure 5B. When the Pica Gene™ Luciferase Control Vector plasmid was used to co-transfect cells with the ribozyme coding sequence plasmid, the luciferase activity (Fig. 5B, lane c) was the same as that obtained by co-transfection with the Pica Gene® Luciferase Control Vector plasmid and the plasmid from which the ribozyme sequence had been deleted (Fig. 5B, lane d), namely no inhibition of luciferase activity was observed (Fig. 5B, lanes c and d). In contrast, when the N-terminal coding *p300–luc* plasmid was co-transfected with the ribozyme coding plasmid (Fig. 5B, lane a), the luciferase activity was almost two orders of magnitude lower than that obtained after co-transfection of the N-terminal coding *p300–luc* plasmid and the plasmid from which the ribozyme sequence had been deleted (Fig. 5B, lane b). In other words, almost complete inhibition of expression of the *p300–luc*iferase fusion gene was observed (Fig. 5B, lanes a and b). These results clearly confirm the specificity of action of the ribozyme constructs on expression of *p300–luc*.

Finally, we examined the dependence on concentration of the inhibition of luciferase activity. As shown in Figure 6, significant inhibition was detectable even when equimolar amounts of template DNAs for the target and the ribozyme were used. Similar results were obtained with the antisense RNA coding plasmid. However, the inactive ribozyme coding plasmid did not have any inhibitory effect (average inhibition 4%).

In conclusion, we have demonstrated that: (i) the *p300–luc* assay system described here is a simple system in which potential target sites can be easily identified; (ii) ribozyme 2 under the control of the pol III ($tRNA^{Val}$) promoter effectively suppressed expression of the *p300–luc* fusion gene (96%). Exploiting these results, we shall now use this ribozyme 2 system to elucidate details of the function of p300 *in vivo*. To this end, we are isolating stable transformants that generate pol III-derived ($tRNA^{Val}$-derived) ribozyme 2 in our laboratory.

ACKNOWLEDGEMENTS

The authors thank Dr Rchard Eckner and Dr David M. Livingston for the gift of pCMVβ p300 and information of the nucleotide sequence of mouse p300 (unpublished data).

REFERENCES

1 Kitabayashi,I., Eckner,R., Arany,Z., Chiu,R., Gachelin,G., Livingston,D.M. and Yokoyama,K. (1995) *EMBO J.*, **14**, 3496–3509.
2 Jacks,T., Fazeli,A., Schmitt,E.M., Bronson,R.T., Goodell,M.A. and Weinberg,R. (1992) *Nature*, **359**, 295–300.
3 Lane,D.P. (1992) *Nature*, **358**, 15–16.
4 Harlow,E., Whyte,P., Franza,B.R. and Schley,C. (1986) *Mol. Cell. Biol.*, **6**, 1579–1589.
5 Wang,H., Rikitake,Y., Carter,M., Yaciuk,P., Abraham,S., Zerler,S. and Moran,E. (1993) *J. Virol.*, **66**, 476–488.
6 Eckner,R., Ewen,M.E., Newsome,D., Gerdes,M., DeCaprio,J.A., Lawrence,J.B. and Livingston,D. (1994) *Genes Dev.*, **8**, 869–884.
7 Arany,Z., Newsome,D., Oldread,E., Livingston,D.M. and Eckner,R. (1995) *Nature*, **374**, 81–84.
8 Arany,Z., Sellers,W.R., Livingston,D.M. and Eckner,R. (1994) *Cell*, **77**, 799–800.
9 Chrivia,J.C., Kwok,R.P.S., Lamb,N., Hagiwara,M., Montminy,M.R. and Goodman,R.H. (1993) *Nature*, **365**, 855–859.
10 Lundblad,J.R., Kwok,R.P.S., Laurance,M.E., Harter,M.L. and Goodman,R.H. (1995) *Nature*, **374**, 85–87.
11 Kwok,R.P.S., Lundblad,J.R., Chrivia,J.C., Richards,J.P., Bachinger,H.P., Brensnan,R.G., Roberts,S.G.E., Green,M.K. and Goodman,R.H. (1994) *Nature*, **370**, 223–226.
12 Abraham,S.E., Lobo,S., Yaciuk,P., Wang,H. and Moran,E. (1993) *Oncogene*, **8**, 1639–1647.
13 Altman,S. (1993) *Proc. Natl. Acad. Sci. USA*, **90**, 10898–10900.
14 Marschall,P., Thompson,J.B. and Eckstein,F. (1994) *Cell. Mol. Neurobiol.*, **14**, 523–538.
15 Murray,J.A.H. (ed.) (1992) *Antisense RNA and DNA*. Wiley-Liss, New York, NY.
16 Erickson,R.P. and Izant,J.G. (eds) (1992) *Gene Regulation: Biology of Antisense RNA and DNA*. Raven Press, New York, NY.
17 Kawasaki,H., Machida,M., Komatsu,M., Li,H., Murata,T., Tsutsui,H., Fujita,A., Matsumura,M., Kobayashi,Y., Taira,K. and Yokoyama,K.K. (1996) *Artificial Organs*, in press.
18 Eckstein,F. and Lilley,D.M.J. (eds) (1996) *Nucleic Acids and Molecular Biology*, Vol. 10. Springer-Verlag, Berlin, Germany.
19 Sun,L.Q., Wang,L., Gerlach,W.L. and Symonds,G. (1995) *Nucleic Acids Res.*, **23**, 2909–2913.
20 Zhao,J.J. and Pick,L. (1993) *Nature*, **365**, 448–451.
21 Feng,M., Cabrera,G., Deshane,J., Scanlon,K.J. and Curiel,D.T. (1995) *Cancer Res.*, **55**, 2024–2028.
22 Uhlenbeck,O.C. (1987) *Nature*, **328**, 596–600.
23 Sheldon,C.C. and Symons,R.H. (1989) *Nucleic Acids Res.*, **17**, 5679 –5685.
24 Forster,A.C. and Symons,R.H. (1987) *Cell*, **49**, 211–220.
25 Haseloff,J. and Gerlach,W.L. (1989) *Gene*, **82**, 43–52.
26 Ohkawa,J., Koguma,T., Kohda,T. and Taira,K. (1995) *J. Biochem.*, **118**, 251–258.
27 Rossi,J. (1995) *TIBTECH*, **13**, 301–306.

28 Bratty,J., Chartrand,P., Ferbeyre,G. and Cedergren,R (1993) *Biochim. Biophys. Acta*, **1216**, 345–359.
29 Piccirilli,J.A., Vyle,J.S., Caruthers,M.H. and Cech,T.R. (1993) *Nature*, **361**, 85–88.
30 Yarus.M. (1993) *FASEB J.*, **7**, 31–39.
31 Uchimaru,T., Uebayasi,M., Tanabe,K. and Taira,K. (1993) *FASEB J.*, **7**, 137–142.
32 Steitz,T.A. and Steitz,J.A. (1993) *Proc. Natl. Acad. Sci. USA*, **90**, 6498–6502.
33 Pyle,A.M. (1993) *Science*, **261**, 709–714.
34 Dahm,S.C., Derrick,W.B. and Uhlenbeck,O.C. (1993) *Biochemistry*, **32**, 13040–13045.
35 Uebayasi,M., Uchimaru,T., Koguma,T., Sawata,S., Shimayama,T. and Taira,K. (1994) *J. Org. Chem.*, **59**, 7414–7420.
36 Sawata,S., Komiyama,M. and Taira,K. (1995) *J. Am. Chem. Soc.*, **117**, 2357–2358.
37 Kumar,P.K.R., Zhou,D.M., Yoshinari,K. and Taita,K. (1996) In Eckstein,F. and Lilley,D.M.J. (eds), *Nucleic Acids and Molecular Biology*, Vol. 10. Springer-Verlag, Berlin, Germany, pp. 217–230.
38 Zhou,D.-M., Usman,N., Wincott,F.E., Matulic-Adamic,J., Orita,M., Zhang,L.-H., Komiyama,M., Kumar,P.K.R. and Taira,K. (1996) *J. Am. Chem. Soc.*, **118**, 5862–5866.
39 Inokuchi,Y., Yuyama,N., Hirashima,A., Nishikawa,S., Ohkawa,J. and Taira,K. (1994) *J. Biol. Chem.*, **269**, 11361–11366.
40 Ruffner,D.E., Stormo,G.D. and Uhlenbeck,O.C. (1990) *Biochemistry*, **29**, 10695–10702.
41 Zoumadakis,M. and Tabler,M. (1995) *Nucleic Acids Res.*, **23**, 1192–1196.
42 Shimayama,T. Nishikawa,S. and Taira,K. (1995) *Biochemistry*, **34**, 3649–3654.
43 Haseloff,J. and Gerlach,W.L. (1988) *Nature*, **334**, 585–591.
44 Lieber,A. and Strauss,M. (1995) *Mol. Cell. Biol.*, **8**, 466–472.
45 Homann,M., Tabler,M., Tzortzakaki,S. and Sczakiel,G. (1994) *Nucleic Acids Res.*, **22**, 3951–3957.
46 Long,D. and Uhlenbeck,O.C. (1994) *Proc. Natl. Acad. Sci. USA*, **91**, 6977–6981.
47 Tang,X., Hobom,G. and Luo,D. (1994) *J. Med. Virol.*, **42**, 385–395.
48 Shimayama,T., Nishikawa,F., Nishikawa,S. and Taira,K. (1993) *Nucleic Acids Res.*, **21**, 2605–2611.
49 Sawata,S., Shimayama,T., Komiyama,M., Kumar,P.K.R., Nishikawa,S. and Taira,K. (1993) *Nucleic Acids Res.*, **21**, 5656–5660.
50 Seiduschek,E.P. and Tocchini,S.P. (1988) *Annu. Rev. Biochem.*, **57**, 873–914.
51 Alam,J. and Cook,J.L. (1990) *Anal. Biochem.*, **188**, 245–254.
52 Chomczynski,P. and Sacchi,N. (1987) *Anal. Biochem.*, **16**, 156–159.
53 McMaster,G.K. and Carmichael,G.G. (1977) *Proc. Natl. Acad. Sci. USA*, **74**, 4835–4838.
54 Hertel,K.J., Pardi,A., Uhlenbeck,O.C. Koizumi,M., Ohtsuka,E., Uesugi,S., Cedergren,R., Eckstein,F., Gerlach,W.L., Hodgson,R. and Symons,R.H. (1992) *Nucleic Acids Res.*, **20**, 3252.
55 Wong-Staal,F. (1995) *Adv. Drug Delivery Rev.*, **17**, 363–368.
56 Cotten,M. and Birnstiel,M.L. (1989) *EMBO J.*, **8**, 3861–3866.